0026-895X/94/020189-12$03.00/0

MOLECULAR PHARMACOLOGY, 45:189-200

Direct Evidence for the Existence and Functional Role of Hyperreactive Sulfhydryls on the Ryanodine Receptor-Triadin Complex Selectively Labeled by the Coumarin Maleimide 7-Diethylamino-3-(4′-maleimidylphenyl)-4-methylcoumarin

GUOHUA LIU, JONATHAN J. ABRAMSON, ANTHONY C. ZABLE, and ISAAC N. PESSAH

Department of Molecular Biosciences, Division of Pharmacology and Toxicology, School of Veterinary Medicine, University of California, Davis, California 95616 (G.L., I.N.P.), and Department of Physics, Portland State University, Portland, Oregon 97207 (J.J.A., A.C.Z.)

Received June 10, 1993; Accepted November 15, 1993

SUMMARY

The fluorogenic sulfhydryl probe 7-diethylamino-3-(4′-maleimidylphenyl)-4-methylcoumarin (CPM) (1–50 nM) is used to characterize the functional role and location of highly reactive thiol groups on the ryanodine-sensitive Ca^{2+} release channel complex [i.e., ryanodine receptors (RyRs)] of skeletal and cardiac junctional sarcoplasmic reticulum (SR). The kinetics of forming fluorescent CPM adducts with junctional but not longitudinal SR membrane proteins (0.02–1 pmol of CPM/μg of SR protein) are found to be markedly dependent on the presence of physiological and pharmacological modulators of the RyR Ca^{2+} channel. RyR agonists, micromolar Ca^{2+}, and nanomolar ryanodine promote a slow SR thiol-CPM reaction, with an apparent rate constant k of 0.0021 ± 0.0002 sec^{-1}, and >89% of the fluorescence is associated with the 110-kDa Ca^{2+} pump, which constitutes 68% of the protein in the SR preparations. However, in the presence of Ca^{2+} channel antagonists (millimolar Mg^{2+}, millimolar Ca^{2+}, or micromolar ryanodine), CPM rapidly forms adducts with a single class of highly reactive (hyperreactive) SR thiols ($k = 0.025 \pm 0.002$ sec^{-1}). Nonreducing sodium dodecyl sulfate-polyacrylamide gel electrophoresis of CPM-labeled SR protein and Western blot analyses with antiryanodine or antitriadin antibodies reveal that the hyperreactive thiols labeled by CPM under conditions favoring channel closure are localized principally to the RyR protomer and triadin, which constitute <6% of the protein in the SR preparation. Immunoprecipitation experiments with antiryanodine and antitriadin monoclonal antibodies confirm the location of CPM-labeled thiol groups on RyR and triadin, respectively. The results indicate that the RyR and triadin contain a small number of highly reactive cysteine residues that selectively conjugate with CPM only when channel closure is favored. It is shown that either 1) the redox state (sulfhydryl/disulfide status) or 2) the accessibility of the hyperreactive thiols on the RyR and triadin is determined by the conformational state of the channel. Covalent modification of hyperreactive thiols with nanomolar CPM inhibits both Ca^{2+}-induced Ca^{2+} release and the gating activity of single channels reconstituted in bilayers, revealing the essential functional importance of hyperreactive thiols on channel-associated proteins. 1,4-Naphthoquinone (0.4–40 pmol/μg of protein) selectively oxidizes hyperreactive thiols on RyR and triadin and releases Ca^{2+} from SR vesicles, without inhibiting Ca^{2+}-ATPase activity. The results provide direct evidence of the existence and functional role of hyperreactive cysteine residues on the RyR and triadin in regulating the gating of ryanodine-sensitive intracellular Ca^{2+} channels and strongly suggest that these important Ca^{2+} regulatory channels may be an important target for oxidative cell damage mediated by quinones.

Ryanodine-sensitive Ca^{2+} release channels (i.e., RyR) are widely expressed in SR/ER membranes of excitable and nonexcitable cells (1–8) and constitute a major site of convergence for signal transduction involving Ca^{2+} (9). In striated muscle, Ca^{2+} stored within SR is released through Ca^{2+}-selective channels in response to depolarization of the T-tubule membrane. L-type, dihydropyridine-sensitive, Ca^{2+} channels within the skeletal T-tubule membrane operate primarily as voltage sensors that mediate movement of gating charge during excitation-contraction coupling (10). In cardiac muscle, L-type Ca^{2+} channels serve primarily as ion-selective channels that regulate Ca^{2+} entry into the myocyte (11). SR Ca^{2+} release channels of

This work was supported by Grant ES05002 and National Institute of Environmental Health Sciences Center for Environmental Health Sciences Grant ES05707 from the National Institutes of Health.

ABBREVIATIONS: RyR, ryanodine receptor; AMP-PCP, β,γ-methyleneadenosine-5′-triphosphate; BLM, bilayer lipid membrane(s); CHAPS, 3-[(3-cholamidopropyl)dimethylammonio]-1-propanesulfonate; CPM, 7-diethylamino-3-(4′-maleimidylphenyl)-4-methylcoumarin; DACM, *N*-(7-dimethylamino-4-methyl-3-coumarinyl) maleimide; ER, endoplasmic reticulum; HEPES, *N*-2-hydroxyethylpiperazine-*N*′-2-ethanesulfonic acid; MOPS, 3-(*N*-morpholino)propanesulfonic acid; NEM, *N*-ethylmaleimide; SR, sarcoplasmic reticulum; FKBP12, 12-kDa FK506-binding protein; NQ, 1,4-naphthoquinone; T-tubule, transverse tubule; SDS, sodium dodecyl sulfate; PAGE, polyacrylamide gel electrophoresis; SH, sulfhydryl; DMSO, dimethylsulfoxide; EGTA, ethylene glycol bis(β-aminoethyl ether)-*N*,*N*,*N*′,*N*′-tetraacetic acid.

skeletal muscle are localized at the junctional face of SR terminal cisternae and comprise the junctional 'feet' structures that span the T-tubule/SR junction. The RyR is composed of four 565-kDa (based on cDNA) protomers (1, 12–14) and tightly associated immunophilin FKBP12 (15). Cardiac Ca^{2+} channels are found at T-tubule/SR junctions and within corbular SR (16). Ca^{2+} channels of skeletal and cardiac muscle bind the plant alkaloid ryanodine with nanomolar affinity and thus have been termed RyRs (17, 18). Because of its complexity, the relationships between RyR structure and the molecular events leading to activation of the Ca^{2+} channels have remained unclear. A number of investigators have reported that SH-oxidizing reagents, including anthraquinones (19, 20), reactive disulfides (21, 22), and heavy metal ions (23), induce the release of Ca^{2+} from SR vesicles and modify the gating behavior of individual Ca^{2+} channels reconstituted in BLM, suggesting that the oxidation state of "critical" SH moieties may be important in regulating the SR Ca^{2+} channel (23–25). However, the identity of the proteins that are the targets of thiol-reactive reagents in the SR membrane has not been clearly established. Whether physiologically relevant modulators of the RyR allosterically alter the thiol redox state of channel-associated proteins is unknown. Direct demonstration of the existence, location, and essential function of critical thiols within the channel protein complex has been lacking. The rationale behind the present studies is that, if redox cycling of SH moieties is essential to normal channel gating, then the critical SHs must surely be chemically reactive to account for the rapidity of channel gating. The nonfluorescent maleimide CPM (Fig. 1) readily undergoes Michael addition with protein thiols, producing an irreversible adduct with high fluorescent yield (26). Using CPM at low concentrations (1–50 nM, i.e., 0.02–1.0 pmol/μg of SR protein), we have examined the kinetics of labeling of junctional SR protein from rabbit skeletal or rat cardiac muscle in the presence of physiologically and pharmacologically relevant channel activators or inhibitors. This report demonstrates 1) the existence of a discrete class ($\leq$1 pmol/μg of SR protein) of highly reactive thiol groups on the SR membrane, 2) that their reactivity is markedly influenced by known physiological and pharmacological modulators of the RyR, 3) that hyperreactive SHs are localized primarily on the RyR protomer and triadin, and 4) that hyperreactive thiols are essential for the normal gating of Ca^{2+} channels. The exquisite sensitivity of the channel thiols towards redox-active toxicants such as NQ, relative to other SR (ER) proteins, strongly suggests that these important Ca^{2+} regulatory channels may be a primary target for oxidative cell damage mediated by quinones.

Experimental Procedures

Preparation of SR. Membrane fractions enriched in terminal cisternae (junctional SR) and longitudinal SR were prepared from rabbit skeletal muscle according to the method of Saito *et al.* (27). Heavy SR from rat cardiac ventricles was prepared by sucrose-density gradient centrifugation, as described previously (20). All membrane preparations (5–8 mg/ml protein) (28) were stored in 10% sucrose, 5 mM imidazole, pH 7.4, at −80°. Unless otherwise noted, SR vesicles were diluted to 50 μg/ml in buffer A (100 mM KCl, 20 mM MOPS, pH 7.0) just before experiments were initiated.

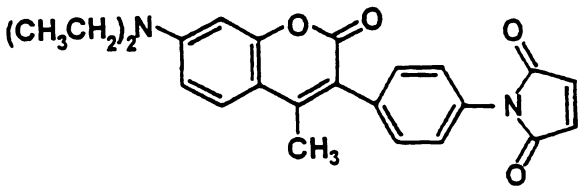

Fig. 1. Structure of CPM.

Fluorescence labeling of SR proteins and fluorometry. CPM (100 μM) dissolved in DMSO was stored at −20° and diluted 10-fold just before use. CPM solutions were protected from light at all times. The maximum volume of DMSO added to SR membranes was limited to 0.5% (v/v) of the assay buffer to ensure that the solvent did not interfere with either fluorescence or normal SR Ca^{2+} release. After incubation of SR vesicles with Ca^{2+} channel modulators in buffer A at 37° for 3 or 5 min, CPM (1–50 nM, i.e., 0.02–1 pmol/μg of protein) was added to the reaction mixture (2-ml final volume) in a thermostatted quartz cuvette. The sample was continuously stirred with an electromagnet having a mixing time of $\leq$2 sec. CPM was added through a small hole in the top of the sample compartment, using a 10-μl Hamilton syringe to minimize mixing artifacts. CPM fluorescence was monitored with a spectrofluorometer (SML 8000; SML Instrument Inc., Urbana, IL) interfaced with an IBM computer/recording system. Excitation and emission wavelengths were set at 397 nm and 465 nm (slit = 16 nm), respectively. Data were sampled at 1 Hz and the rates of increasing fluorescence were analyzed by nonlinear regression analysis (ENZFITTER; Elsevier BioSoft).

Analysis of fluorescent thiol-labeling kinetics. The time course of fluorescence intensity (F) obtained in the presence of channel inhibitors (see legends to Figs. 3 and 6) can be described by

$$F = F_{max}\,[1 - \exp(-kt)] \quad (1)$$

Differentiating Eq. 1 yields

$$dF/dt = kF_{max}\exp(-kt) \quad (2)$$

where F_{max} is the maximum fluorescence intensity and k is the rate constant of increasing fluorescence and is directly related to CPM-thiol binding. Because of the bimolecular covalent nature of the binding reaction, the rate of CPM binding to thiol (SH) groups and the rate of CPM fluorescence development can be expressed, respectively, as

$$d[\text{CPM-SH}]/dt = k_m[\text{SH}][\text{CPM}] \quad (3)$$

and

$$dF/dt = Qk_m[\text{SH}][\text{CPM}] \quad (4)$$

The molecular binding rate constant k_m reflects the apparent reactivity of the SH groups, and [SH] and [CPM] are the free concentrations of SH and CPM, respectively, at time t. Q is the fluorescence quantum yield. At the initial instant of CPM binding $R_i = dF/dt$ ($t \rightarrow 0$), and Eqs. 2 and 4 can be written, respectively, as

$$R_i = kF_{max} \quad (5)$$

and

$$R_i = Qk_m[\text{SH}]_t[\text{CPM}]_t \quad (6)$$

$[\text{CPM}]_t$ is the total CPM concentration added, and $[\text{SH}]_t$ is the initial concentration of free SH groups. Using k and F_{max} values obtained from kinetic measurements of CPM fluorescence labeling of free thiols, the initial rate, R_i, can be calculated (Eq. 5). Based on Eq. 6, plotting R_i against $[\text{CPM}]_t$ gives the slope

$$S = Qk_m[\text{SH}]_t \quad (7)$$

Combining Eqs. 5 and 6, and substituting $Q = F_{max}/[\text{CPM}]_t$ (because there is no detectable free CPM after fluorescence intensity reaches a maximum value; see Results), yields

$$k = k_m[\text{SH}]_t \quad (8)$$

Therefore, the rate constant (k) associated with development of fluorescence upon conjugation of CPM with free thiols is dependent on

1) the k_m, which reflects the inherent reactivity of SR thiols, and 2) the total number of available SH groups on the SR membrane, $[SH]_t$.

SDS-PAGE. Thirty milliliters of SR protein (50 μg/ml) were incubated with channel modulators in buffer A at 37° for 3 min. After exposure of SR membranes to 50 nM (1.0 pmol/μg of protein) CPM for 1 min, 2 mM NEM was added to quench the reaction. SR vesicles were centrifuged at 190,000 × *g* for 3 hr at 4°. The whole pellets were resuspended in 1 ml of buffer A, the protein concentration was determined (28), and protein was solubilized (1:1) with nonreducing sample buffer (48 mM NaH_2PO_4, 170 mM Na_2HPO_4, 6 M urea, 0.02% bromphenol blue, 1%, w/v, SDS). The samples were incubated at 37° for 2 min and 20 μg of protein were loaded onto a 4–20% gradient SDS-polyacrylamide gel (29) and electrophoresed at constant voltage (200 V). The fluorescent protein bands on the gel were visualized at 360-nm excitation using a transilluminator and the fluorescence image was photographed through a 450-nm cutoff filter. The fluorescence intensity of protein bands was digitized by a video analysis system (Jandel Scientific) and integrated by computer within the linear range of protein density.

Western blot analysis. The protein bands resolved by SDS-PAGE were transferred to polyvinylidene difluoride microporous membranes by electroblotter (Mini Trans-Blot; Bio-Rad) overnight at 30 V (4°) and for 1 hr at 100 V. Blotted polyvinylidene difluoride membranes were incubated for 1 hr with 5 μg/ml mouse anti-rabbit triadin monoclonal antibody GE4.90 (30) or with a 1/100 dilution of mouse anti-RyR monoclonal antibody 34C (31) in phosphate buffer, pH 7.4, with 3% bovine serum albumin. The immunoblots were incubated with biotinylated anti-mouse IgG for 30 min and with horseradish peroxidase conjugated with biotin/avidin (VECTASTAIN ABC kit; Vector Labs, Burlingame, CA) for an additional 30 min. Color was developed using 3,3′,5,5′-tetramethylbenzidine substrate (Vector).

Immunoprecipitation. Immunoprecipitation experiments were performed as reported previously (12, 13), with slight modifications. Agarose beads with covalently attached goat anti-mouse IgG antibodies (Sigma Chemcial Co., St. Louis, MO) were washed with buffer B (0.5 M NaCl, 10 mM sodium phosphate, pH 7.4) and incubated at 4° overnight with buffer C (0.15 M NaCl, 10 mM sodium phosphate, pH 7.4) containing 0.010–0.5 mg/ml affinity-purified anti-RyR monoclonal antibody 34C (31) or anti-rabbit triadin monoclonal antibody GE4.90 (30). The beads were washed three times with 1 ml of buffer B and incubated for 36 hr at 4° with CHAPS-solubilized junctional foot protein prelabeled with CPM or [^{3}H]ryanodine. For these experiments, prelabeling of SR (1 mg/ml) with CPM was conducted in the presence of 1 mM $MgCl_2$ plus 100 μM EGTA (channel closed) or 100 μM $CaCl_2$ plus 200 nM NQ (channel activated) in buffer A for 3 min, followed by addition of 1 pmol of CPM/μg of protein for 1 min and addition of 5 mM NEM. For [^{3}H]ryanodine binding, SR protein was incubated with 100 nM [H^3]ryanodine (specific activity, 68 Ci/mmol; New England Nuclear) for 10 min. CPM- or [^{3}H]ryanodine-prelabeled SR was solubilized for 2 hr at 37° in a solution consisting of 1 M NaCl, 1.6% CHAPS, 1 mM phenylmethylsulfonyl fluoride, and 20 mM MOPS, pH 7.0,. The solutions were centrifuged at 1000 × *g* for 2 min at 4°, and the supernants were decanted and saved for analysis. The pellets were resuspended and pelleted three times in ice-cold buffer B. The fluorescence intensity of the immunoprecipitates and supernatants was measured immediately. The [^{3}H]ryanodine specifically bound to the immunoprecipitate was quantified by liquid scintillation counting. The proteins concentrated (by Speed VAC centrifugation) from supernatant fractions after immunoprecipitation were denatured in nonreducing SDS sample buffer and run on a 3–10% SDS-polyacrylamide gel.

Ca^{2+} transport. SR protein (250 μg/ml) was treated first with 5 mM Mg^{2+} and then for 1 min with or without CPM in buffer A (described above). The mixture was diluted 5-fold with a transport buffer consisting of 92 mM KCl, 20 mM K-MOPS, pH 7.0, 7.5 mM sodium pyrophosphate, and 250 μM antipyrylazo III. MgATP (1 mM), 10 μg/ml creatine phosphokinase, and 5 mM phosphocreatine (an ATP-regenerating system) were added and Ca^{2+} fluxes were monitored at 740–790 nm, using a diode-array spectrophotometer (model 8452A; Hewlett Packard). Raw data were collected digitally and analyzed by nonlinear regression analysis.

Measurement of Ca^{2+}(Mg^{2+})-ATPase. Ca^{2+}-dependent ATPase activity was measured spectrophotometrically by enzymatically coupling ADP production to the oxidation of NADH with phosphoenolpyruvate, pyruvate kinase, and lactate dehydrogenase (32).

Single-channel records in BLM. The SR Ca^{2+} release channel was reconstituted in BLM (50 mg/ml phosphatidylethanolamine/phosphatidylserine, 5:3, in decane). SR vesicles suspended in 0.3 M sucrose were added to the *cis* chamber (final SR protein concentration, 5–10 μg/ml) of the BLM apparatus. The *cis* chamber contained 500 mM CsCl, 0.3–0.7 mM $CaCl_2$, 5 mM HEPES, pH 7.2, whereas the *trans* chamber contained 100 mM CsCl, 5 mM HEPES, pH 7.2. After a single-step-like fusion event, an excess of EGTA, pH 7.2, was added to the *cis* chamber, which was subsequently perfused with an identical buffer with no added Ca^{2+} or EGTA. All current recordings were measured with respect to the *trans* side (i.e., the ground side), at +25-mV holding potential with respect to the *trans* (ground) side, with asymmetric Cs^+ (500 mM *cis*, 100 mM *trans*), as reported previously (33). Picoampere currents were amplified (Warner Instruments Bilayer Clamp) and digitized without filtering.

Results and Discussion

Kinetics of CPM labeling of SR membranes are markedly dependent on SR Ca^{2+} channel modulators. The basic behavior of CPM and GSH and the resultant fluorescence increase in the presence or absence of SR Ca^{2+} channel modulators are examined in Fig. 2. The formation of CPM-thiol adducts with GSH in standard assay buffer A results in an immediate increase in fluorescence intensity, which rapidly reaches a stable maximum when all CPM in the cuvette is conjugated with GSH (Fig. 2A, *0 mM* NEM trace). However, if GSH (2 mM) is pretreated with a molar excess of NEM (5 mM), subsequent addition of 50 nM CPM results in only a small increase in fluorescence intensity due to very minor autofluorescence of CPM (Fig. 2A, *5 mM* NEM trace), which has been subtracted from all experiments shown below. Addition of $CaCl_2$ (10 μM to 2 mM), $MgCl_2$ (≤10 mM), ryanodine (10 nM to 300 μM), or neomycin (50 nM to 300 μM) after adduct formation is complete does not significantly alter the intensity of CPM fluorescence (Fig. 2A). Similar results are observed with GSH if channel modulators are added before introduction of CPM. The rate of fluorescence development and the maximal fluorescence intensity of CPM-GSH thiol adducts are completely insensitive to the presence of $CaCl_2$, $MgCl_2$, or ryanodine (Fig. 2B). These control experiments demonstrate that differences in the patterns of fluorescence developed in the presence of native SR and various Ca^{2+} channel modulators shown in subsequent experiments are not the result of a trivial change in the fluorescence yield due to quenching of CPM fluorescence and/or increases in autofluorescence. To examine whether channel modulators alter the affinity of thiol groups for CPM, SR protein was denatured with 5% SDS at 100° for 10 min and then treated with $CaCl_2$ or $MgCl_2$ for 3 min (Fig. 3A). No difference is observed in the rate of CPM fluorescence development in the presence of channel activators (100 μM Ca^{2+} plus 100 nM ryanodine) or the channel inhibitor Mg^{2+} (10 mM). In addition, the binding kinetics of CPM with denatured SR are also insensitive to other modulators of SR Ca^{2+} channels (data not shown). In marked contrast, native skeletal SR membranes pretreated with 100 μM Ca^{2+} and 100 nM ryanodine result in a slow rate of fluorescence increase upon addition of CPM,

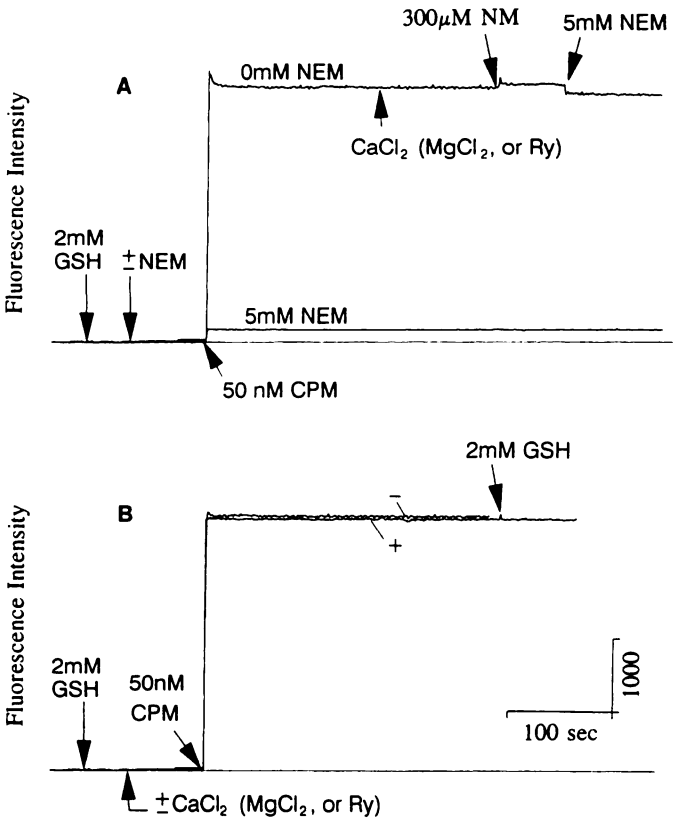

Fig. 2. GSH thiol selectivity and fluorescence of CPM-thiol adducts are unaffected by Mg^{2+} and Ca^{2+}. A, GSH (2 mM) was pretreated with (+) or without (−) 5 mM NEM in buffer A containing 100 mM KCl and 20 mM MOPS, pH 7.0. CPM (50 nM) was added to the mixture and increasing fluorescence was monitored with time at 37°, using a spectrofluorometer set at 465 nm (emission) and 397 nm (excitation) (see Experimental Procedures). For NEM-untreated SR (*0 mM* NEM trace), after the fluorescence intensity reached a constant value $CaCl_2$ (5 μM to 2 mM), $MgCl_2$ (0.2–10 mM), ryanodine (*Ry*) (10 nM to 300 μM), 300 μM neomycin (*NM*), or 5 mM NEM was added. B, GSH (2 mM) was preincubated with (+) or without (−) $CaCl_2$, $MgCl_2$, or ryanodine, at ranges of concentration described in A, before addition of CPM (50 nM) to the reaction medium. The experiment was repeated at least three times.

whereas 10 mM Mg^{2+} dramatically increases the rate of CPM fluorescence (Fig. 3B). The data presented above provide the first evidence that the rate of formation of thiol-CPM adducts on native junctional SR membranes is markedly influenced by physiologically relevant SR Ca^{2+} channel modulators. Longitudinal SR preparations, which lack RyR, calsequestrin, and triadin (Fig. 4A, compare *lane 2* with *lane 3*), exhibit CPM labeling kinetics that are sensitive to neither Ca^{2+} nor Mg^{2+} (Fig. 4B), strongly suggesting that proteins localized to the junctional SR membrane are responsible for the observed sensitivity of CPM labeling to known physiological modulators of the Ca^{2+} release channel.

Fig. 5 shows that the rate of CPM labeling of native junctional SR is dependent on the concentration of Ca^{2+} or Mg^{2+} in the assay medium. After 3-min preincubation of skeletal SR membranes (50 μg/ml protein) with various concentrations of Ca^{2+} or Mg^{2+}, addition of 10 nM CPM (i.e., 0.2 pmol/μg of protein) results in a time-dependent increase in fluorescence intensity. Under conditions known to promote SR Ca^{2+} channel activation (50 μM Ca^{2+}), the rate of labeling of SR thiols with CPM proceeds slowly, with an apparent rate constant (k) of 0.0027 ± 0.0002 sec^{-1} ($t_{1/2} = 257 \pm 18$ sec, six experiments). An assay condition that favors channel closure (10 mM Mg^{2+}) increases the kinetics of CPM binding to SR protein by >10-fold ($k = 0.028 \pm 0.002$ sec^{-1}, $t_{1/2} = 24.8 \pm 1.7$ sec, six experiments) (Fig. 5A). Increasing Ca^{2+} from 7 μM (the level of free Ca^{2+} normally introduced with SR) to 50 μM (by addition of $CaCl_2$) results in dose-dependent decreases in the rate of CPM binding, paralleling SR Ca^{2+} channel activation. In contrast, increasing Mg^{2+} (1–10 mM) or Ca^{2+} (≥300 μM), conditions that promote channel closure, dramatically enhances the rate of development of CPM fluorescence (Fig. 5A). The predictable nature of the binding of CPM to SR protein also extends to known pharmacological modulators of the SR Ca^{2+} release channel. The known Ca^{2+} channel activators caffeine, AMP-PCP, and doxorubicin promote "slow" CPM labeling kinetics, whereas inhibitors of the channel such as ruthenium red, neomycin, and FLA365 result in rapid labeling kinetics (data not shown). The sensitivity of CPM kinetics to the channel modulators extends to cardiac SR membranes. Micromolar Ca^{2+} or NQ, a potent activator of SR Ca^{2+} channels (as shown below), decreases, whereas millimolar Ca^{2+}, millimolar Mg^{2+}, or lowered free Ca^{2+} (≤4.3 nM with 0.5 mM EGTA) (34) increases, the rate of CPM binding to the membrane proteins (Fig. 6). Significant is the observation that both Ca^{2+} (Figs. 5A and 6) and ryanodine (Fig. 7), which have biphasic actions on SR Ca^{2+} channel function (35, 36), also induce biphasic labeling kinetics with CPM. Fig. 7 illustrates the biphasic nature of the CPM binding rate constant (k) in the presence of nanomolar to micromolar concentrations of ryanodine. For example, ryanodine (5–50 nM) stabilizes an open state of the skeletal SR Ca^{2+} channel, enhancing open probability (33), and significantly slows CPM labeling kinetics. In contrast, high concentrations (>100 μM) of ryanodine close the Ca^{2+} channel (35, 36) and increase the rate of CPM binding to protein thiols (Fig. 7). Taken together, these results demonstrate that physiologically and pharmaco-

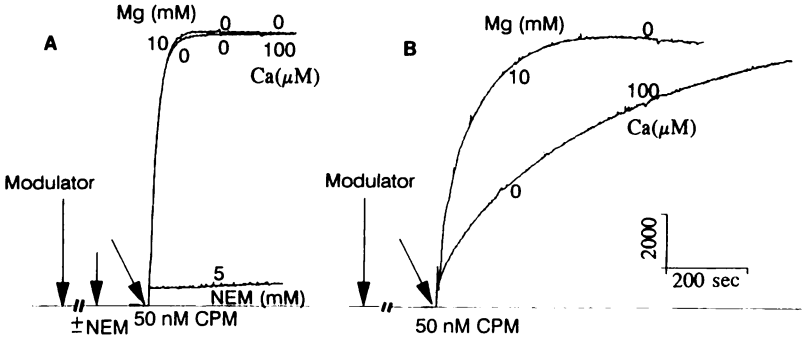

Fig. 3. Ca^{2+} and Mg^{2+} modulate the rate of CPM-thiol adduct formation with native but not denatured SR. A, Junctional skeletal SR (5 mg/ml) was denatured in 5% SDS buffer at 100° for 10 min. B, Native junctional SR membranes were used. All samples (50 μg/ml protein) were preincubated with or without 100 μM $CaCl_2$ plus 100 nM ryanodine, 10 mM $MgCl_2$, or 5 mM NEM. CPM (50 nM) was added to the mixture and fluorescence intensity was monitored as described in Fig. 1. The experiment was repeated at least three times.

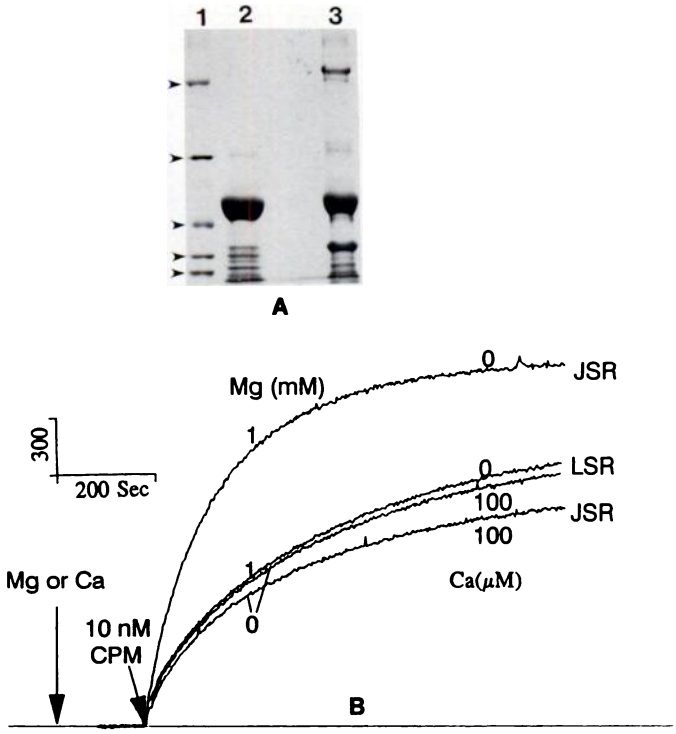

Fig. 4. CPM labeling of longitudinal SR deficient in RyR, calsequestrin, and triadin is insensitive to Mg^{2+} and Ca^{2+}. In A, 30 μg of longitudinal SR (*lane 2*) or junctional SR (*lane 3*) were loaded onto a 3–10% nonreducing SDS gel. *Lane 1*, standard markers (M_r 340,000, 170,000, 85,600, 59,000, and 39,000, in order from *top* to *bottom*). In B, SR protein [junctional SR (*JSR*) or longitudinal SR (*LSR*), 50 μg/ml] was pretreated with Mg^{2+} (1 mM) or Ca^{2+} (100 μM) plus ryanodine (100 nM) for 3 min at 37° in buffer A. Increasing CPM (10 nM) fluorescence was monitored as described for Fig. 3. The experiment was repeated three times for each longitudinal SR preparation. Three different longitudinal SR preparations were examined.

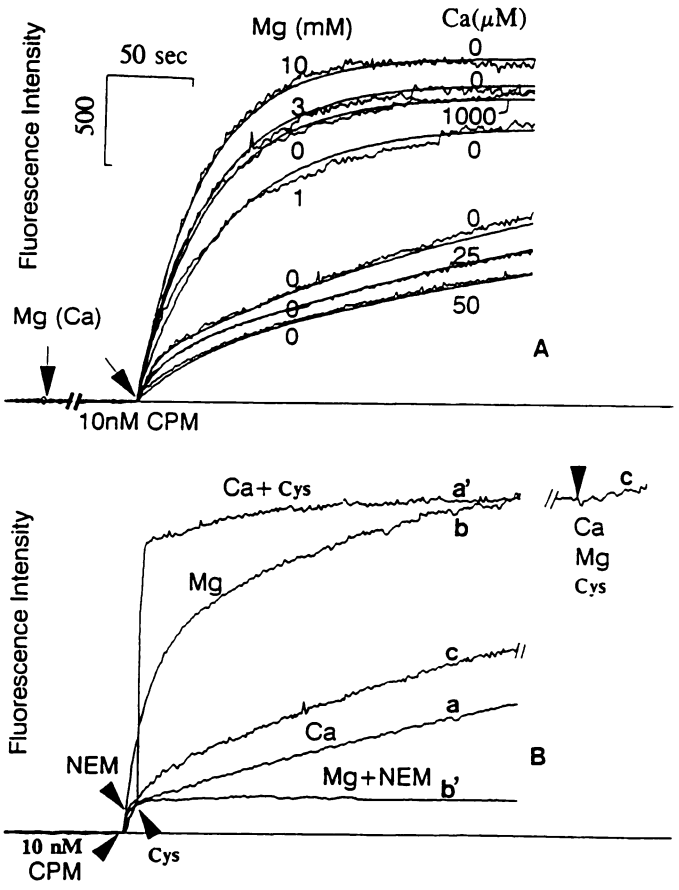

Fig. 5. The rate of fluorescence development resulting from labeling of junctional SR thiols with CPM is dependent on the concentration of known modulators of the RyR of skeletal muscle. Millimolar Mg^{2+} or Ca^{2+} enhances, whereas micromolar Ca^{2+} decreases, the rate of CPM labeling of SR thiols. A, Aliquots (2 ml) of skeletal junctional SR (50 μg/ml protein) were individually exposed at 37° for 3 min to the final concentrations of $CaCl_2$ or $MgCl_2$ in a buffer solution containing 100 mM KCl and 20 mM MOPS, pH 7.0,. CPM (10 nM, i.e., 0.2 pmol/μg of protein) was then added to the mixture. The fluorescence development was monitored as described for Fig. 1. The data were fit using the equation $F = F_{max}[1 - \exp(-kt)]$ (*uppermost trace*, 10 mM Mg^{2+}) or double-exponential functions (*other traces*), as shown by the *smooth curves*. B, Ten seconds after addition of CPM to 50 μM Ca^{2+}-incubated membranes, 0 (*trace a*) or 1 mM cysteine (*Cys*) (*trace a'*) was applied. Five seconds after addition of CPM to 10 mM Mg^{2+}-incubated SR vesicles, 0 (*trace b*) or 2 mM NEM (*trace b'*) was added. After fluorescence intensity reached the maximum in the absence of added $CaCl_2$ or $MgCl_2$ (*trace c*), 10 mM $MgCl_2$, 50 μM $CaCl_2$, or 1 mM cysteine was added to the reaction mixture. The lack of any change in fluorescence yield upon addition of SR Ca^{2+} channel modulators to CPM-labeled SR demonstrates an insensitivity of the probe to channel conformation when this reaction scheme is used. The data shown are representative of at least three experiments.

logically relevant modulators acting at various effector sites markedly alter the kinetics of CPM binding to SR thiols.

Why do channel modulators change the rate constant of CPM labeling of native junctional SR thiol groups? In the absence of native SR, Mg^{2+} and Ca^{2+} do not influence the affinity of protein thiols for CPM, nor do they alter the fluorescent quantum yield, because neither ion alters the fluorescence behavior of the CPM-GSH or the CPM-SR (denatured) complex in the assay buffer used (Figs. 2 and 3A). Therefore, the dramatic increase in the rate constant (k) of CPM binding to SR thiols in the closed state of the channel, compared with the activated state, could be the result of either 1) an increase in the fluorescence quantum yield (Q) of bound CPM on the native SR membranes (Eqs. 4 and 6; see Experimental Procedures), which could be caused by changes in molecular microenvironment around the CPM-SH complex, 2) a marked increase in the total number of thiol groups on the SR membranes that are available for CPM labeling ($[SH]_t$) (Eq. 8; see Experimental Procedures), or 3) a dramatic increase in the reactivity (k_m) of one or more classes of thiols (k_m, in eq. 8) when the SR Ca^{2+} channels are in the closed conformation. If possibility 1 is true, then addition of Mg^{2+} or Ca^{2+} after CPM labeling reaches completion should result in a change in the fluorescence intensity in a manner similar to that observed when the SR is pretreated with these ions. However, addition of either Mg^{2+} or Ca^{2+} to the CPM-labeled SR membranes once the free CPM is fully consumed (ensured by addition of an excess of cysteine at the end of the experiment) does not alter the fluorescence maxima (Fig. 5B, *trace c*). In fact, addition of 1 mM cysteine 10 sec after addition of CPM to the Ca^{2+}-activated SR membranes quickly increases CPM fluorescence intensity to the same maximum (Fig. 5B, *trace a'*), indicating that most of the CPM is not bound to SR protein thiols when the Ca^{2+} channels are activated. However, addition of 2 mM NEM to Mg^{2+}-incubated membranes (Fig. 5B, *trace b'*) completely stops CPM binding to reactive SR thiols by directly competing with CPM for those groups. The fact that the final fluorescence intensity (F_{max}) reaches the same value regardless of the presence of Mg^{2+} or

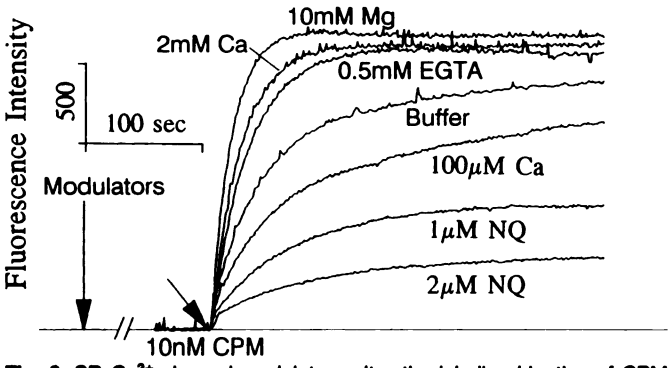

Fig. 6. SR Ca^{2+} channel modulators alter the labeling kinetics of CPM with rat cardiac SR. Micromolar Ca^{2+} and NQ decrease, whereas millimolar Ca^{2+} and Mg^{2+} increase, the rate of CPM binding to rat cardiac SR thiols. Cardiac SR (50 μg/ml) was incubated at 37° with or without the indicated channel modulators for 5 min before addition of CPM (10 nM) in buffer A, and fluorescence was measured as described for Fig. 1. The experiment was repeated twice and gave essentially the same results.

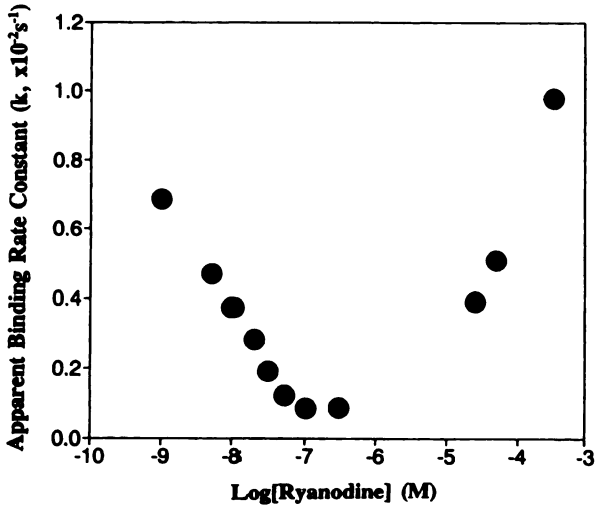

Fig. 7. Ryanodine alters the apparent binding rate constant (k) of CPM for skeletal SR hyperreactive thiol groups, in a biphasic manner. In the presence of 20 μM Ca^{2+}, skeletal SR (50 μg/ml protein) was incubated with various concentrations of ryanodine for 5 min. The time course of increasing fluorescence upon addition of CPM (10 nM, i.e., 0.2 pmol/μg of protein) was recorded as described in Experimental Procedures. The apparent rate constant (k) was calculated from the half-time ($t_{1/2}$) to achieve the maximum fluorescence intensity. Data shown are the mean obtained from three independent experiments.

Ca^{2+} (compare Fig. 5B, *traces b* and *c*) further demonstrates that the two ions do not change the fluorescence yield in the presence of native SR membranes. A plot of final fluorescence intensity (F_{max}) versus CPM (1–50 nM) reveals a linear relationship with a slope, representing fluorescence yield (Q), of 203.5 ± 8 and 202.2 ± 5 nM^{-1} in the presence of 10 mM $MgCl_2$ or 100 μM Ca^{2+} plus 100 nM ryanodine, respectively (Fig. 8).

Taken together, these results suggest that differences in CPM labeling kinetics either are due to a change in the total number of SR thiols ($[SH]_t$) available for forming adducts with CPM or are the result of a marked change in the reactivity (k_m) of one or more classes of SR thiols. Clearly, the CPM-thiol adducts formed under the present labeling protocols, and thus fluorescence quantum yield (Q), are not sensitive to conformational changes induced by physiologically relevant channel modulators. In this respect the present studies are markedly

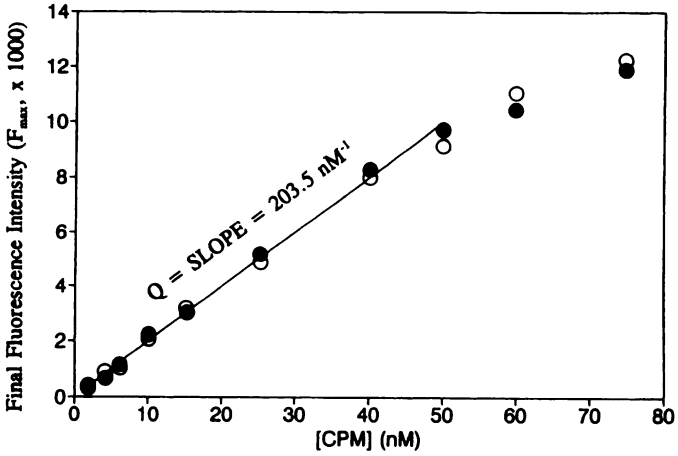

Fig. 8. Mg^{2+} and Ca^{2+} do not influence the fluorescent yield (Q) of native SR membranes labeled with CPM (≤50 nM). SR (50 μg/ml protein) was pretreated for 3 min at 37° with 10 mM Mg^{2+} (●) or 100 μM Ca^{2+} plus 100 nM ryanodine (○) in buffer A. The indicated concentration of CPM was added to skeletal SR membranes and fluorescence was monitored as described for Fig. 1. The final fluorescence intensity values (F_{max}) were taken directly from time courses shown in Fig. 7, at the maximum value reached for each corresponding concentration of CPM. The least-squares linear regression line for the pooled data has an r^2 value of 0.99. Data points above 50 nM CPM deviate from linearity because long (~1-hr) incubation times are needed to fully consume the excess free CPM with less reactive SR thiols, thereby resulting in some photobleaching.

different from those previously reported by Ikemoto and coworkers with a related probe, DACM (37, 38). In those studies, micromolar DACM and labeling conditions were used in which the conformational state of the channel was undefined. Previous strategies for fluorescence labeling of SR protein thiols have added DACM and SR before known channel modulators are added to the reaction medium (24, 37, 38). Addition of various channel modulators after labeling is complete has revealed a 10–15% change in fluorescence intensity, which is probably due to a change in the fluorescent yield (Q) of the DACM-thiol adducts in response to changes in the local conformation of the release channel (24, 37, 38). The labeling strategy presented here uses physiological and/or pharmacological modulators of the channel before introduction of 0.02–1 pmol of CPM/μg of SR protein. Under the present conditions, fluorescent yield (Q) of adducts formed between CPM and a small number of thiols (see below) on the SR membrane is insensitive to channel conformation once adduct formation is complete.

Although the rate constant k of CPM binding to thiols on native SR increases directly with increasing Mg^{2+} (1–10 mM) (Fig. 5A) or other channel inhibitors (e.g., ruthenium red or neomycin) (data not shown), k is independent of CPM concentration (1–50 nM) at a constant concentration of Mg^{2+} (10 mM) and the curves describing fluorescence development are perfectly fit by a single-exponential function, $F(t) = F_{max}[1 - \exp(-k_{closed}t)]$, having a mean k_{closed} at 1–50 nM CPM of 0.025 ± 0.002 sec^{-1} (Fig. 9A). However, the time course of fluorescence development obtained under conditions in which a large fraction of channels are activated (e.g., 100 μM Ca^{2+} plus 100 nM ryanodine) (Fig. 9B) is best fit by a double-exponential function, $F(t) = F_{closed}[1 - \exp(-k_{closed}t)] + F_{open}[1 - \exp(-k_{open}t)]$. The first phase, $F_{closed}[1 - \exp(-k_{closed}t)]$, is characterized by having a k value (0.029 sec^{-1}) similar to that (k_{closed}; see above) obtained in the presence of 10 mM Mg^{2+}. However,

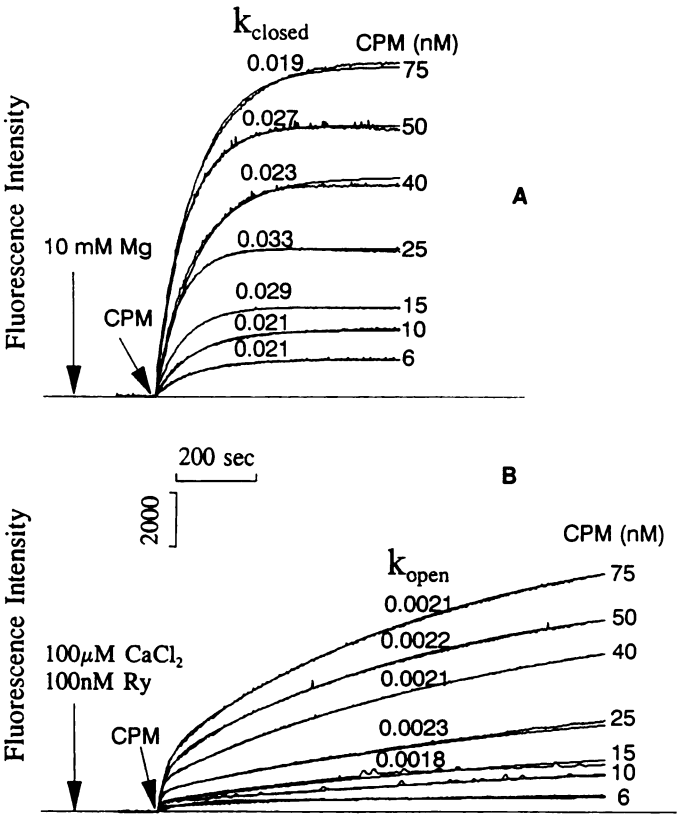

Fig. 9. The rate constant k of thiol fluorescent labeling of SR protein is independent of the CPM concentration but is sensitive to Mg^{2+} or Ca^{2+} at a range of CPM concentrations of ≤50 nM. SR (50 μg/ml protein) was incubated with 10 mM Mg^{2+} (A) or 100 μM Ca^{2+} plus 100 nM ryanodine (*Ry*) (B) for 3 min. The indicated concentration of CPM (6–75 nM, i.e., 0.12–1.5 pmol/μg of protein) was applied to the membranes. In A, the time courses of increasing fluorescence in the presence of Mg^{2+} were best fit by a single-exponential function of time t, $F(t) = F_{max}[1 - \exp(-k_{closed}t)]$ (k_{closed} = 0.025 ± 0.002 sec^{-1}, averaged over all CPM concentrations of ≤50 nM). In B, the data in the presence of SR Ca^{2+} channel activators were best fit by a double-exponential function, $F(t) = F_{closed}[1 - \exp(-k_{closed}t)] + F_{open}[1 - \exp(-k_{open}t)]$ (k_{closed} = 0.029 ± 0.003 sec^{-1}, k_{open} = 0.0021 ± 0.0002 sec^{-1}, and $F_{open} \approx 8 \times F_{closed}$; average of all CPM concentrations used). The *upper trace* (75 nM CPM) in A was fit by a double-exponential function containing a major component $F_{closed}[1 - \exp(-k_{closed}t)]$, with a k_{closed} value similar to those of other traces in A, and a minor component having a slow rate constant (k = 0.0015 sec^{-1}). *Numbers above each curve*, actual k value.

in the presence of channel activators the magnitude of F_{closed} is minor and it makes a small contribution to overall fluorescence (Fig. 9B). In contrast, the second phase ($F_{open}[1 - \exp(-k_{open}t)]$) has a >10-fold slower rate constant (mean k_{open} at 1–50 nM CPM = 0.0021 ± 0.0002 sec^{-1}), comprises the major component of fluorescence, and is likely associated with a large population of less-reactive thiols on the SR membrane, because $F_{open} \gg F_{closed}$. To further illustrate the significant impact of SR Ca^{2+} channel modulators on CPM kinetics, a plot of the initial rate of CPM fluorescence (R_i) versus total CPM concentration, according to $R_i = kF_{max}$ (Eq. 5), is shown in Fig. 10. The linear relationships between R_i and $[CPM]_t$ under conditions known to activate or inhibit the channel clearly demonstrate that the theoretical treatment on which the principle of CPM-SH reaction kinetics is based (Eq. 6; see Experimental Procedures) is compatible with the experimental results. It is likely that, under conditions promoting the closed or open conformation of the channel, the product of $[SH]_t$, k_m, and Q is statistically

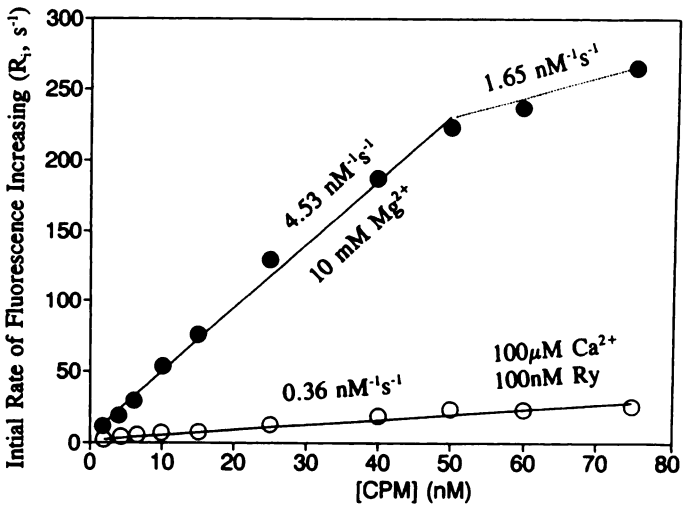

Fig. 10. Initial rates (R_i) of fluorescence plotted against CPM concentration indicate that the slope ($Qk_m[SH]_t$) in the presence of SR Ca^{2+} channel inhibitors is significantly greater than that observed in the presence of SR Ca^{2+} channel activators. The initial rate R_i was calculated from k and F_{max} (from Fig. 9) using the equation $R_i = kF_{max}$ (eq. 5 in Experimental Procedures). For Mg^{2+}-treated SR k_{closed} was used as the k value, whereas for Ca^{2+}-incubated membranes k in eq. 5 was substituted with k_{open}. The final fluorescence intensity (F_{max}) was taken from each trace at the maximum value. *Ry*, ryanodine.

constant, as reflected by the slope $S = Qk_m[SH]_t$ (Fig. 10). Obviously, the slope S_{closed} in the presence of 10 mM Mg^{2+} is significantly greater then S_{open} in the presence of 100 μM Ca^{2+} plus 100 nM ryanodine. That is, S_{closed} is >10 times S_{open} or $(Qk_m[SH]_t)_{closed}$ is >10 times $(Qk_m[SH]_t)_{open}$. Because the quantum yield (Q) of CPM fluorescence is insensitive to channel modulators under the conditions used, it follows that $(k_m[SH]_t)_{closed}$ is much larger than $(k_m[SH]_t)_{open}$. Therefore, the difference observed between S_{closed} and S_{open} (and hence k_{closed} and k_{open}; see Eq. 8) is the result of a change in 1) thiol reactivity (k_m) or 2) the total number of SR thiols available for CPM binding ($[SH]_t$). More information about how k_m and $[SH]_t$ contribute to the markedly different labeling kinetics observed can be obtained by identifying which SR proteins are fluorescently labeled by CPM, using SR pretreated with known RyR/Ca^{2+} channel modulators.

Hyperreactive SR thiols are localized on the SR Ca^{2+} channel complex. Labeling with 50 nM CPM (i.e., 1 pmol/μg of protein) in an assay medium known to promote channel activation reveals that >89% of the total fluorescence developed is incorporated into the 110-kDa Ca^{2+}-dependent ATPase (Fig. 11, A, *lane 2*, and B, *Ca trace*). This finding is not surprising, because the Ca^{2+} pump is the major protein component, comprising ~68% of total protein in the present SR preparation, and contains ~26 thiols/Ca^{2+}-ATPase molecule (39). However, when the channel is closed with 10 mM Mg^{2+} (Fig. 11, A, *lane 3*, and B, *Mg trace*) or 500 μM neomycin (40) (Fig. 11, A, *lane 4*, and B, *NM trace*), minimal fluorescence is detected for the ATPase band. Instead, 93% of the total fluorescence is associated with the RyR protomer (M_r 360,000 band that cross-reacts with the anti-RyR monoclonal antibody; data not shown) and bands of M_r 95,000, 39,500, and 12,500 that constitute ~6% of the total protein in the SR preparation. A 95-kDa glycoprotein, termed triadin, has been identified by Caswell *et al.* (30) and recently cloned (41); it appears to form an association with the RyR and has been suggested to play a structural role in coupling

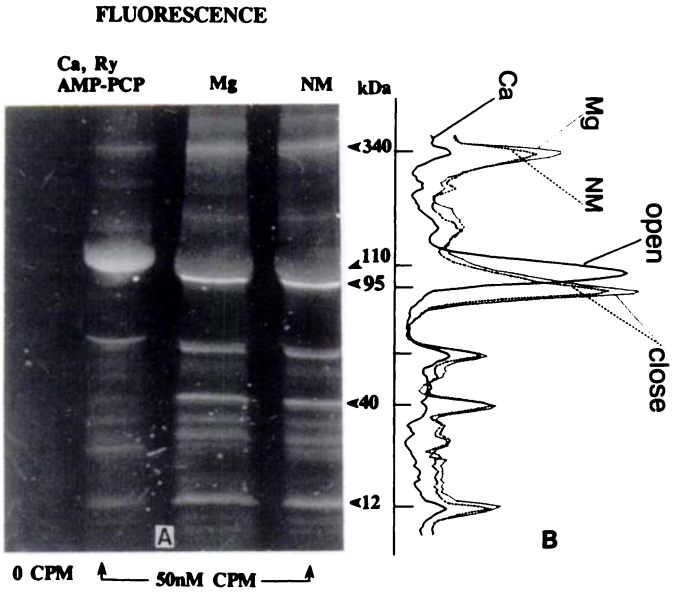

Fig. 11. SR Ca^{2+} channel modulators dramatically influence the pattern of fluorescently CPM-labeled SR proteins in SDS-PAGE. A, Image of a nonreducing SDS-PAGE gel of CPM-labeled skeletal junctional SR protein, as seen by transilluminator. B, Plot of the relative fluorescence intensity of the protein bands after digitization, as described in Experimental Procedures. SR protein (50 μg/ml) was incubated for 3 min at 37° with buffer alone (*lane 1*, numbered from *left*), 100 μM Ca^{2+}, 1 mM AMP-PCP, and 50 nM ryanodine (*Ry*) (*lane 2*), 10 mM Mg^{2+} (*lane 3*), or 500 μM neomycin (*NM*) (*lane 4*), in the same buffer solution described in the legend to Fig. 1. Each SR sample (except *lane 1*, which served as an autofluorescence control) was exposed to 50 nM (1.0 pmol/μg of protein) CPM for 1 min, followed by addition of 2 mM NEM to quench the reaction (see Experimental Procedures). Twenty micrograms of protein were loaded onto each lane of a 4–20% gradient SDS-polyacrylamide gel. Consistent with the slower kinetics of CPM labeling of SR in the presence of SR Ca^{2+} channel activators, the total integrated fluorescence intensity in *lane 2* is 50% of that found in *lanes 3* and *4* (in the presence of channel inhibitors). This experiment was repeated at least five times.

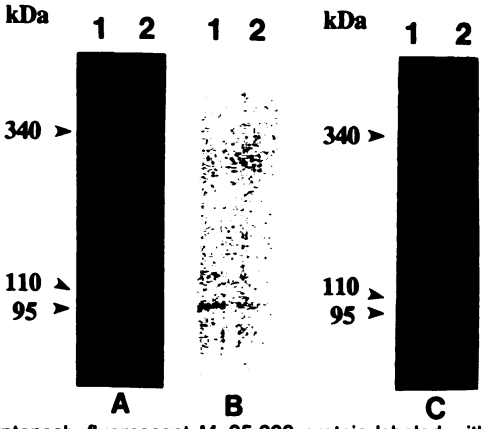

Fig. 12. Intensely fluorescent M_r 95,000 protein labeled with CPM (A, *lane 1*) stains with antitriadin antibody on Western blots when SR is inactivated before SDS-PAGE separation (B, *lane 1*). In C, a fluorescence image demonstrates the selective oxidation by NQ of thiols on M_r 360,000, and 95,000 proteins. Skeletal SR protein (2 mg/ml) was incubated for 3 min at 37° with 10 mM $MgCl_2$ plus 0.2 mM EGTA (A and B, *lanes 1*), 100 μM $CaCl_2$ plus 50 nM ryanodine and 1 mM AMP-PCP (A and B, *lanes 2*), 0.5 mM EGTA (C, *lane 1*), or 0.5 mM EGTA plus 10 pmol/μg of SR protein of NQ (C, *lane 2*). The membranes were exposed to CPM (0.5 pmol/μg of protein) for 1 min, followed by addition of 2 mM NEM and denaturation with a nonreducing SDS sample buffer. Thirty micrograms of protein were loaded onto each lane of a 3–10% gradient SDS-polyacrylamide gel. Western blotting was performed as described in Experimental Procedures.

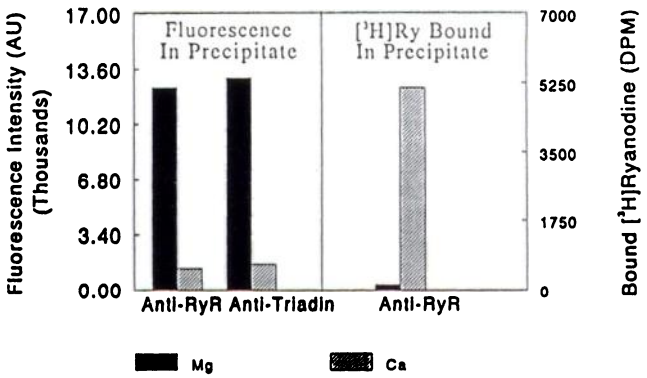

Fig. 13. CPM-labeled junctional SR proteins are immunoprecipitated by anti-RyR and antitriadin monoclonal antibodies. Skeletal SR protein (1 mg/ml) was incubated for 3 min at 37° with 1 mM $MgCl_2$ plus 100 μM EGTA or 100 μM $CaCl_2$ plus 200 nM NQ (an SR Ca^{2+} channel activator; see Fig. 14). CPM (1 pmol/μg of protein) was added to the mixture, followed by addition of 5 mM NEM. SR used for immunoprecipitation of [^{3}H]ryanodine binding sites was incubated for 10 min with 100 nM [^{3}H] ryanodine (*[^{3}H]Ry*) instead of CPM. After solubilization with 1.6% (w/v) CHAPS, immunoprecipitation with anti-RyR and antitriadin antibodies was performed (see Experimental Procedures). The immunoprecipitates were washed three times and the pellets were measured fluorometrically or by liquid scintillation counting. Data are presented as flourescence intensity found in the pellets. The experiment was repeated three times with the same results.

L-type Ca^{2+} channels of the T-tubule membrane with the SR Ca^{2+} release channel (42). The intensely fluorescent band labeled by CPM at M_r 95,000 in the present study (Fig. 12A, *lane 1*) strongly cross-reacts with antitriadin antibodies on Western blots (Fig. 12B, *lane 1*). Ca^{2+} channel inhibition also significantly increases the amount of CPM-labeled thiols associated with minor protein bands at M_r 39,500 and 12,500 whose identities remain to be determined. Aldolase, which has been shown to bind to the junctional foot protein and to be released by inositol polyphosphates, has a molecular weight of 40,000 (43). Further, the major cytoplasmic form of FKBP12 in human T cells has recently been shown to be tightly associated with the RyR of skeletal muscle (15, 44), in a ratio of >1 molecule/functional Ca^{2+} channel (15). Based on cDNA, each FKBP12 polypeptide contains a single cysteine residue (15). Positive identification of the CPM-labeled bands at M_r 39,500 and 12,500 remains to be elucidated.

To ensure that the proteins rapidly labeled with CPM in the presence of channel inhibitors are associated with RyR and triadin, immunoprecipitation experiments with anti-RyR and antitriadin antibodies were performed with CPM-prelabeled SR proteins (Fig. 13). SR prelabeled with CPM under conditions promoting channel closure (10 mM Mg^{2+}) contains a significantly higher fluorescence in the immunoprecipitate, compared with SR pretreated in the presence of channel activators. Immunoprecipitation of [^{3}H]ryanodine binding sites in samples prelabeled under channel-activating conditions verifies that RyRs are indeed immunoprecipitated (Fig. 13). As expected, the supernatants collected after immunoprecipitation (and concentration) no longer show the bright fluorescent bands at M_r 360,000 or 95,000. These results confirm that thiol groups on the RyR and triadin are avialable for CPM labeling only when channel inactivation is favored.

Together, the kinetic and SDS-PAGE data show that activation of the channel permits CPM to slowly label mainly the

abundant ATPase thiols, whereas closure of the channel allows CPM to rapidly bind to the RyR subunit and associated proteins such as triadin. Under the present labeling conditions only a small fraction of SR thiols, representing considerably less than 1% of the total SR thiols ($[SH]_t$) in the membrane preparation, are labeled by CPM at completion of the reaction. Thus, the marked increase in the rate of formation of CPM adducts with the Ca^{2+} channel-associated proteins seen in the presence of channel inhibitors (Fig. 11) represents binding to a very small number of thiols, relative to the total number ($[SH]_t$) of SR thiols. The only plausible explanation is that RyR-associated protein thiols must have a much greater reactivity than do other (more abundant) SR protein thiols (i.e., $k_{m\text{-channel}} \gg k_{m\text{-other}}$), only in an environment that promotes channel closure. Therefore, the thiols on the RyR channel complex are "hyperreactive," relative to other SR thiols, and selectively bind CPM (1–50 nM) when the closed conformation of the channel is favored. Concentrations of CPM of >50 nM indeed give biexponential rates despite the presence of channel inhibitors (Fig. 9A, *upper trace*), and the relationship between R_i and $[CPM]_t$ deviates from linearity (Fig. 10, *dashed line*, above 50 nM CPM). This is not surprising, because formation of CPM adducts with SR protein is a bimolecular irreversible reaction and the finite number of hyperreactive thiols associated with SR Ca^{2+} channel proteins appear to be saturated with 1 pmol of CPM/μg of SR protein. CPM at >50 nM would be expected to label more abundant but much less reactive SR thiols. Why does CPM label channel-associated proteins only under conditions favoring the closed conformation of the channel? This can be explained by either 1) the closed state of the channel having increased accessibility to a small finite number of hyperreactive thiols or 2) channel modulators altering the redox state (SH/S-S) of these hyperreactive thiols on the channel complex. In this respect it is important to note that CPM readily crosses biological membranes and would be expected to rapidly gain access to thiols localized at hydrophilic and hydrophobic regions of the SR Ca^{2+} channel complex.

Hyperreactive thiols on the SR Ca^{2+} channel are exquisitely sensitive to the redox environment. The involvement of SH oxidation in SR Ca^{2+} channel activation is clearly demonstrated with NQ, a potent SH-oxidizing reagent. NQ (2 μM, 0.04 nmol/μg of protein) added to Ca^{2+}-loaded SR vesicles induces release of accumulated Ca^{2+} through a pathway inhibited by ruthenium red (Fig. 14A, *trace b*). NQ does not inhibit the Ca^{2+} pump (confirmed by reuptake of Ca^{2+} upon the addition of ruthenium red). NQ is ineffective in releasing Ca^{2+} from the SR when the hyperreactive thiols have been covalently prelabeled with CPM (data not shown), suggesting that NQ induces Ca^{2+} release via an oxidation reaction of hyperreactive SH groups. To confirm this concept, 50 μg/ml SR protein was treated with NQ (2 μM) for 3 min. As shown in Fig. 14B, pretreatment with NQ dramatically suppresses the rate of CPM binding to the membranes. Further, CPM no longer labels the proteins of M_r 360,000 and 95,000 when exposed to NQ (1.0 pmol/μg of SR protein), despite conditions that promote SR Ca^{2+} channel closure (0.5 mM EGTA) (Fig. 12C, compare *lanes 1* and *2*). In contrast, Ca^{2+}-ATPase thiols are still available for CPM labeling in the presence of NQ (Fig. 12C, *lane 2*), thereby demonstrating that the redox state of ATPase thiols remains unaltered. The ability of NQ to selectively alter the redox state of the SR Ca^{2+} channel complex has been observed at concentrations below 100 nM (<2 pmol/μg of SR protein), indicating that functionally important hyperreactive thiols on the Ca^{2+} channel protomer and triadin are exquisitely sensitive to direct redox modification. In fact, both the oxidation of hyperreactive thiols and Ca^{2+} release induced by NQ occur at a level of extravesicular Ca^{2+} (Fig. 14A, $[Ca]_{free} < 1$ μM after loading; Fig. 12C and Fig. 14B, *trace b*, $[Ca]_{free} = 0.0043$ μM) less than that required to trigger Ca^{2+}-induced Ca^{2+} release (Fig. 14A, *trace a*). This indicates that oxidation of the hyperreactive thiols by NQ results in activation of the Ca^{2+} release channel, probably by oxidation of hyperreactive thiols to disulfides. The toxic actions of NQ (and other quinones of toxicological relevance) have been closely associated with their ability to alter Ca^{2+} homeostasis, and oxidation of critical cellular thiols is thought to play an important role (45, 46). Using the CPM assay, the exquisite sensitivity of SR Ca^{2+} channels to chemically induced redox damage is revealed and the specific mechanisms can now be examined in detail. Nanomolar to micromolar levels of NQ also alter specific [^{3}H]ryanodine binding to the channel complex in a potent biphasic manner, whereas naphthalene (the parent structure) is inactive at the receptor (data not shown).

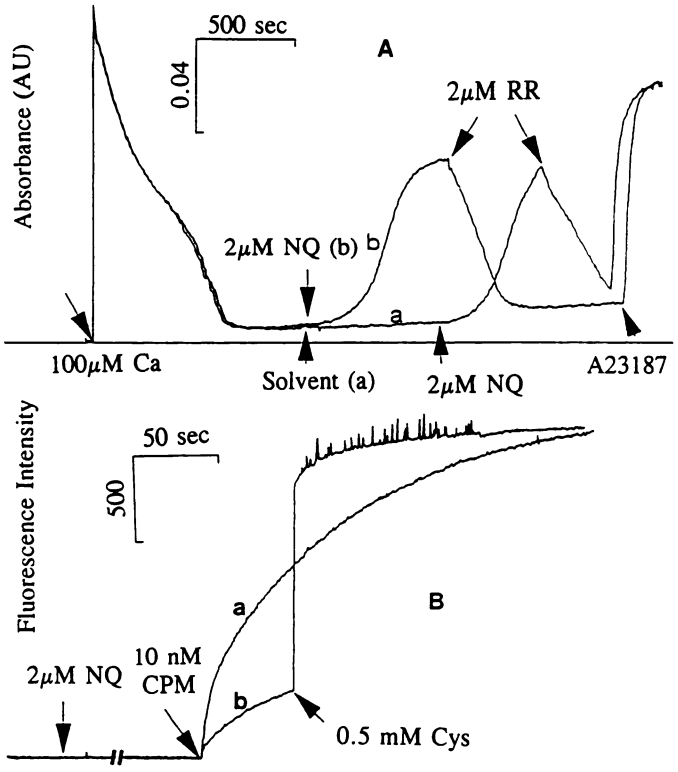

Fig. 14. NQ induces release of Ca^{2+} from skeletal SR vesicles without inhibiting pump activity (A) and oxidizes hyperreactive thiols on the SR membrane (B). A, After loading of 100 μM Ca^{2+} in antipyrylazo III buffer, as described in Experimental Procedures, SR vesicles (50 μg) were exposed to 5 μl of solvent (DMSO) (*trace a*) or 2 μM NQ (*trace b*). Ruthenium red (*RR*) (2 μM) added after initiation of Ca^{2+} release blocks the channel and permits rapid reaccumulation of Ca^{2+}. At the end of each experiment A23187 was added to each cuvette and known additions of Ca^{2+} were used to calibrate the dye signal. B, Skeletal SR (50 μg/ml) was pretreated with 5 μl of DMSO (*trace a*) or 2 μM NQ (*trace b*) for 3 min (*first arrow*), in the same buffer as described for Fig. 1. Each sample received 10 nM CPM (0.2 pmol/μg of protein) and fluorescence was recorded. In *trace b*, 0.5 mM cysteine (*Cys*) was added 50 sec after addition of CPM.

Hyperreactive thiols of the SR Ca^{2+} release channel

complex are critical for channel function. Could the hyperreactive thiol groups of the RyR (and triadin) be critical to SR Ca^{2+} channel function? To answer this question, Ca^{2+} transport studies were conducted under active loading conditions in the presence of pyrophosphate (47). SR membrane vesicles (250 μg/ml protein) in buffer A containing 5 mM Mg^{2+} were exposed to CPM (0.6–1.0 pmol/μg of protein) for 1 min and immediately diluted 5-fold in transport buffer, and active loading of Ca^{2+} was commenced with a single addition of 80 μM $CaCl_2$. Pretreatment of SR membranes with CPM enhances the rate of Ca^{2+} uptake in a dose-dependent manner ($t_{1/2}$ of 483 ± 10 sec for untreated SR and 316 ± 9 sec and 215 ± 12 sec with 40 and 50 nM CPM treatment, respectively) (Fig. 15A). The enhancement of Ca^{2+} uptake by CPM is not the result of enhanced Ca^{2+} pump activity, because the presence of the channel blocker ruthenium red in the CPM-treated membranes does not enhance the rate of Ca^{2+} uptake beyond that seen with control vesicles in the presence of ruthenium red alone (Fig. 15B). In fact, pretreatment of SR with CPM (up to 50 nM, 1 pmol/μg of protein) under these conditions does not alter Ca^{2+}-dependent ATPase activity (3.9 ± 0.3 and 4.1 ± 0.1 μmol/mg/min for control, five experiments, and 50 nM CPM, four experiments, respectively). Labeling of hyperreactive SR thiols with nanomolar CPM does not alter Ca^{2+} uptake with 11 sequential additions of 20 nmol of Ca^{2+} in the loading phase. However, CPM labeling under these conditions inhibits Ca^{2+}-induced Ca^{2+} release initiated by bolus addition of 50 nmol of Ca^{2+}, in a dose-dependent manner (Fig. 15C). Treatment of SR membranes with CPM-cysteine adduct (formed in the presence of 1000-fold excess cysteine) does not inhibit Ca^{2+}-induced Ca^{2+} release, demonstrating that CPM-SR thiol adducts are essential for the actions of CPM on Ca^{2+} transport.

The inhibitory effect of CPM-thiol adducts on Ca^{2+} channel activity is also observed at the level of single channels reconstituted in BLM. After fusion of SR vesicles containing one or two active channels, the Ca^{2+} concentration on the *cis* (cytoplasmic face) side of the BLM was buffered to <100 nM with EGTA. Under these conditions the P_o of the channel averages <0.05. CPM (20 nM) was added to the *cis* chamber and allowed to incubate with the closed channel for approximately 10 min. Upon addition of 50 μM Ca^{2+} to the *cis* side, the open probability increases and rapid discrete fluctuations having a unitary conductance of 468 pS are observed (Fig. 16A, *trace 1*). Occasionally two channels are open at the same time (Fig. 16A, *trace 1, upper dashed line*). An additional 50 μM Ca^{2+} on the *cis* side further activates the channel transiently (Fig. 16A, *trace 2*) but the channel proceeds to inactivate and lock in the closed state (Fig. 16A, *traces 2-6*). Closure of the native (not CPM-modified) SR Ca^{2+} channel in the presence of 100 μM Ca^{2+} on the *cis* side, under the present BLM conditions, has not been observed with several dozen control bilayers. The CPM modification of the gating behavior of the channel is irreversible, because subsequent reperfusion of the *cis* chamber with an identical buffer lacking the maleimide does not alter the CPM-modified channel. CPM (10–20 nM) added directly to the *cis* chamber containing 100 μM Ca^{2+} (i.e., a very active channel) results in a dramatic slowing of single-channel fluctuations, with a lag of 5–10 min after CPM addition (Fig. 16B). A control trace (100 μM Ca^{2+}) typically lasting 5 sec contains approximately 9000 discrete fluctuations, <5 of which last >20 msec. However, upon channel modification by 10 nM CPM a typical trace lasting 20 sec (~5000 fluctuations) contains approximately 400 transitions lasting >20 msec. Within 5 min of CPM modification, the channel locks in a closed conformation and ceases to gate (Fig. 16B). These dramatic irreversible effects of CPM on the gating behavior of the SR Ca^{2+} channel appear to have a slower onset in BLM experiments, compared with fluorescence and transport paradigms. This finding is not surprising, considering the bimolecular nature of formation of CPM-channel adducts. Indeed, the binding of nanomolar CPM to hyperreactive thiols on a single (or at most two) channel in the BLM would be expected to delay the kinetics, compared with the fluorescence and transport assays, which utilize a large population of channels in the respective measurements. The kinetics of labeling of hyperreactive thiols with CPM in the presence of SR Ca^{2+} channel inhibitors are also markedly temperature dependent (data not shown), and this factor also would be expected to contribute to a slower time course for channel modification in BLM studies (performed at 25°). Despite the kinetic limitations imposed by the BLM technique, Michael

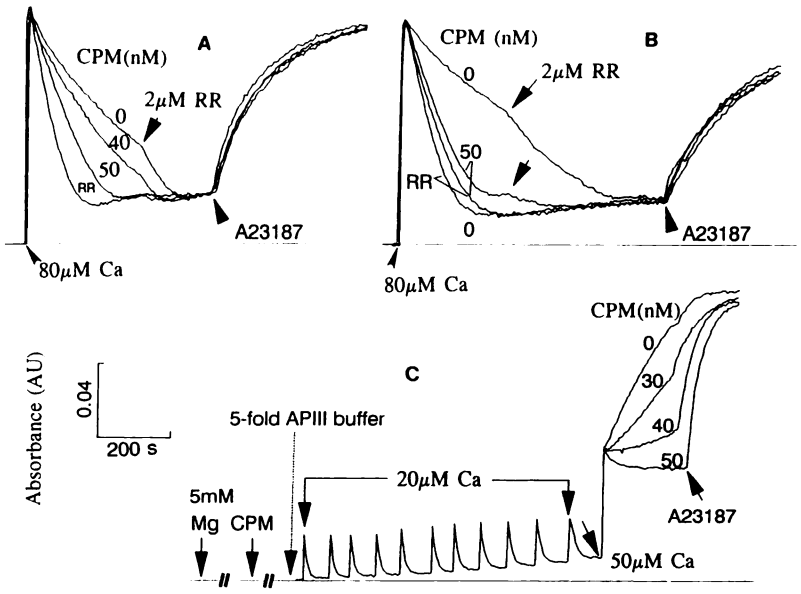

Fig. 15. Pretreatment of SR with CPM enhances Ca^{2+} uptake into rabbit skeletal SR vesicles (A and B) and inhibits Ca^{2+}-induced Ca^{2+} release (C). SR protein (250 μg/ml) was treated first with 5 mM Mg^{2+} and then with the indicated final concentrations of CPM, as described in Experimental Procedures. The mixture was diluted 5-fold with transport assay buffer containing 92 mM KCl, 20 mM K-MOPS, pH 7.0, 7.5 mM sodium pyrophosphate, and 250 μM antipyrylazo III (*APIII*). MgATP (1 mM), 1 mg/ml creatine phosphokinase, and 0.25 M phosphocreatine (an ATP-regenerating system) were added and Ca^{2+} fluxes were monitored. In A and B, ruthenium red (*RR*) (2 μM) was added (*downward arrows*) during the Ca^{2+} uptake phase or before Ca^{2+} loading was begun (*traces RR*). Ionophore A23187 (2 μg) was added at the end of each experiment to ensure equal Ca^{2+} loading of the vesicles and to calibrate the dye.

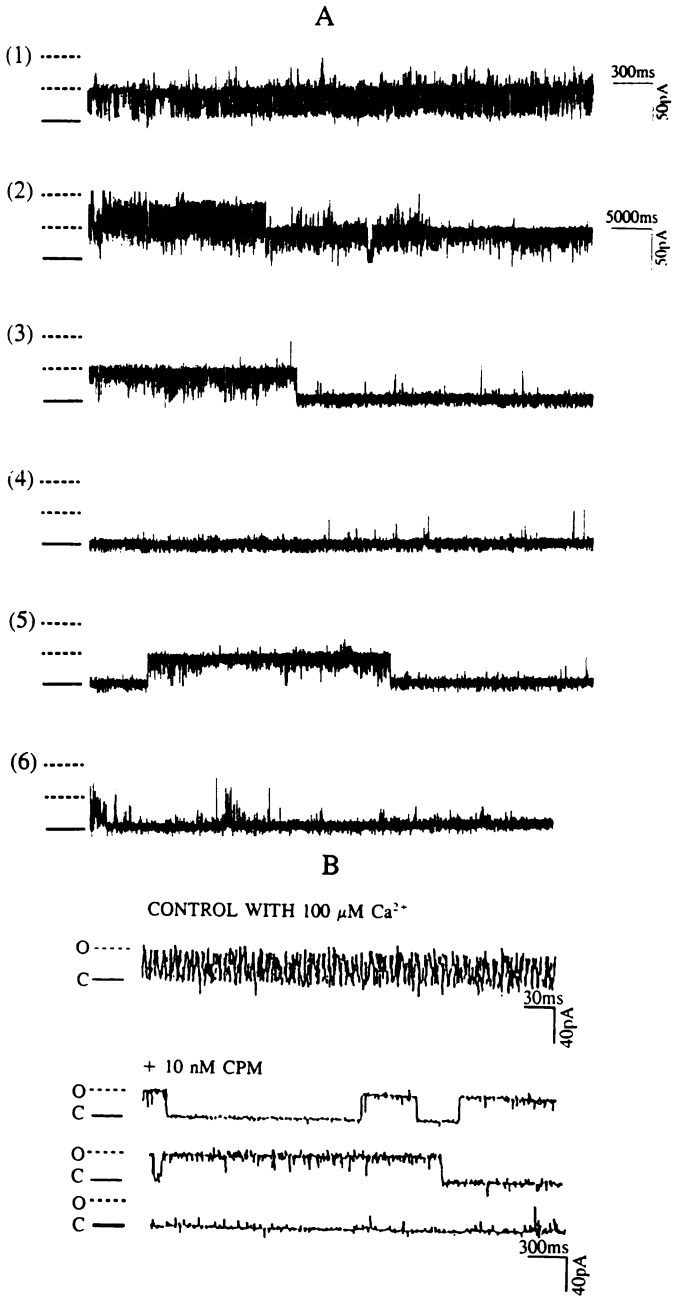

Fig. 16. Nanomolar CPM dramatically alters single-channel gating behavior. A, After fusion of rabbit skeletal SR vesicles to a BLM, the *cis* chamber was perfused with a solution containing 50 μM EGTA in the standard buffer containing 500 mM CsCl, as described in Experimental Procedures. CPM (20 nM) was added and incubated for 5–10 min at ~25°. *Trace 1*, 50 μM $CaCl_2$ was added to the *cis* chamber and current was continuously monitored (3.6 sec/trace). *Traces 2-6*, approximately 5 min of continuous recording (~60 sec/trace) after elevation of the *cis* Ca^{2+} concentration to 100 μM. The open probabilities for the $N = 2$ channels are as follows: *trace 1*, $NP_o = 0.80$; *trace 2*, $NP_o = 0.95$; *trace 3*, $NP_o = 0.40$; *trace 4*, $NP_o < 0.05$. The unitary conductance for the channels shown is ~468 pS (*dashed lines*) and the closed state of the channel is represented by the *solid line*. The time base shown in *trace 2* applies to *traces 2-6*. The behavior of the CPM-modified channel shown was observed in 15 independent BLM experiments. B, CPM (10 nM) added directly to a rapidly fluctuating channel dramatically slowed the gating transitions. *Upper trace*, normal channel-gating events in the presence of 100 μM $CaCl_2$, with 0.5-msec mean open time and conductance of 460 pS. The CPM-modified channel in the presence of 100 μM Ca^{2+} exhibited markedly slower gating kinetics and eventual inactivation. These observations were seen in 12 independent BLM experiments. *O*, open; *C*, closed.

adducts formed between CPM and an individual SR Ca^{2+} channel are readily demonstrated in BLM experiments and attest to the highly reactive nature of thiols critical to the function of SR Ca^{2+} channels.

In conclusion, the present study provides the first direct evidence for the existence of hyperreactive thiols on ryanodine-sensitive Ca^{2+} channel complexes of SR from striated muscle. The formation of covalent CPM adducts with these hyperreactive thiols potently inhibits Ca^{2+} channel activation. A class of hyperreactive thiols on the RyR and its associated proteins appear to be essential for normal channel function. Physiologically and pharmacologically relevant Ca^{2+} channel activators and inactivators acting at a number of sites allosteric to the hyperreactive SH moieties identified in the present study may modulate the redox state of these critical thiols. The present results strongly suggest that redox reactions within or between the RyR oligomer and triadin represent key molecular events in SR Ca^{2+} channel gating. CPM is a valuable probe to study the structure and function of ryanodine-sensitive Ca^{2+} channels and provides a novel method for identifying the location of hyperreactive thiols within the primary sequences of SR Ca^{2+} channel-associated proteins.

Acknowledgments

We thank Drs. A. H. Caswell and J. L. Sutko for generously providing the antitriadin and anti-RyR monoclonal antibodies, respectively, Dr. W. S. Smith for ATPase measurements, and M. M. Mack and M. Schiedt for preparing junctional SR.

References

1. Takeshima, H., S. Nishimura, T. Matsumoto, H. Ishida, K. Kangawa, N. Minamino, H. Matsuo, M. Ueda, M. Hanaoka, T. Hirose, and S. Numa. Primary structure and expression from complementary DNA of skeletal muscle ryanodine receptor. *Nature (Lond.)* **339**:439–445 (1989).
2. Marks, A. R., P. Tempst, K. S. Hwang, M. B. Taubman, M. Inui, C. Chadwick, S. Fleischer, and B. Nadal-Ginard. Molecular cloning and characterization of the ryanodine receptor/junctional channel complex cDNA from skeletal muscle sarcoplasmic reticulum. *Proc. Natl. Acad. Sci. USA* **86**:8683–8687 (1989).
3. Otsu, K., H. F. Willard, V. K. Khanna, F. Zorzato, N. M. Green, and D. H. MacLennan. Molecular cloning of cDNA encoding the Ca^{2+} release channel (ryanodine receptor) of rabbit cardiac muscle sarcoplasmic reticulum. *J. Biol. Chem.* **265**:13472–13483 (1990).
4. Zorzato, F., J. Fujii, K. Otsu, M. Phillips, N. M. Green, F. A. Lai, G. Meissner, and D. H. MacLennan. Molecular cloning of cDNA encoding human and rabbit forms of the Ca^{2+} release channel (ryanodine receptor) of skeletal muscle sarcoplasmic reticulum. *J. Biol. Chem.* **265**:2244–2256 (1990).
5. Nakai, J., T. Imagawa, Y. Hakamat, M. Shigekawa, H. Takeshima, and S. Numa. Primary structure and functional expression from cDNA of the cardiac ryanodine receptor/calcium release channel. *FEBS Lett.* **271**:169–177 (1990).
6. Giannini, G., E. Clementi, R. Ceci, G. Marziali, and V. Sorrentino. Expression of a ryanodine receptor-Ca^{2+} channel that is regulated by TGF-*beta*. *Science (Washington D. C.)* **257**:91–94 (1992).
7. McPherson, P. S., Y. K. Kim, H. Valdivia, C. M. Knudson, H. Takekura, C. Franzini-Armstrong, R. Coronado, and K. P. Campbell. The brain ryanodine receptor: a caffeine-sensitive calcium release channel. *Neuron* **7**:17–25 (1991).
8. Lai, F. A., M. Dent, C. Wickenden, L. Xu, G. Kumari, M. Misra, H. B. Lee, M. Sar, and G. Meissner. Expression of a cardiac Ca^{2+}-release channel isoform in mammalian brain. *Biochem. J.* **288**:553–564 (1992).
9. Berridge, M. J. Calcium oscillations. *J. Biol. Chem.* **265**:9583–9586 (1990).
10. Rios, E., J. J. Ma, and A. Gonzalez. The mechanical hypothesis of excitation-contraction (EC) coupling in skeletal muscle. *J. Muscle Res. Cell Motil.* **12**:127–135 (1991).
11. Fabiato, A., and F. Fabiato. Calcium release from the sarcoplasmic reticulum. *Circ. Res.* **40**:119–129 (1977).
12. Lai, F. A., H. P. Erickson, E. Rousseau, Q. Y. Liu, and G. Meissner. Purification and reconstitution of the calcium release channel from skeletal muscle. *Nature (Lond.)* **331**:315–319 (1988).
13. Imagawa, T., J. S. Smith, R. Coronado, and K. P. Campbell. Purified ryanodine receptor from skeletal muscle sarcoplasmic reticulum is the Ca^{2+}-permeable pore of the calcium release channel. *J. Biol. Chem.* **262**:16636–16643 (1987).
14. Inui, M., A. Saito, and S. Fleischer. Isolation of the ryanodine receptor from cardiac sarcoplasmic reticulum and identity with feet structures. *J. Biol. Chem.* **262**:1740–1747 (1987).
15. Jayaraman, T., A. M. Brillantes, A. P. Timerman, S. Fleischer, H. Erdjument-

Bromage, P. Tempst, and A. R. Marks. FK506 binding protein associated with the calcium release channel (ryanodine receptor). *J. Biol. Chem.* **267**:9474–9477 (1992).
16. Jorgensen, A. O., A. C. Shen, W. Arnold, P. S. McPherson, and K. P. Campbell. The Ca^{2+}-release channel/ryanodine receptor is localized in junctional and corbular sarcoplasmic reticulum in cardiac muscle. *J. Cell Biol.* **120**:969–980 (1993).
17. Pessah, I. N., A. L. Waterhouse, and J. E. Casida. The calcium-ryanodine receptor complex of skeletal and cardiac muscle. *Biochem. Biophys. Res. Commun.* **128**:449–456 (1985).
18. Pessah, I. N., A. O. Francicni, D. J. Scales, A. L. Waterhouse, and J. E. Casida. Calcium-ryanodine receptor complex: solubilization and partial characterization from skeletal muscle junctional sarcoplasmic reticulum. *J. Biol. Chem.* **261**:8643–8648 (1986).
19. Abramson, J. J., E. Buck, G. Salama, J. E. Casida, and I. N. Pessah. Mechanism of anthraquinone-induced calcium release from skeletal muscle sarcoplasmic reticulum. *J. Biol. Chem.* **263**:18750–18758 (1988).
20. Pessah, I. N., E. Durie, M. J. Schiedt, and I. Zimanyi. Anthraquinone sensitized Ca^{2+} release channel from rat cardiac sarcoplasmic reticulum: possible receptor mediated mechanism of doxorubicin cardiomyopathy. *Mol. Pharmacol.* **37**:503–514 (1990).
21. Pessah, I. N., R. A. Stambuk, and J. E. Casida. Ca^{2+}-activated ryanodine binding: mechanism of sensitivity and intensity modulation by Mg^{2+}, caffeine, and adenine nucleotides. *Mol. Pharmacol.* **31**:232–238 (1987).
22. Zaidi, N. F., C. F. Lagenaur, J. J. Abramson, I. N. Pessah, and G. Salama. Reactive disulfides trigger Ca^{2+} release from sarcoplasmic reticulum via an oxidation reaction. *J. Biol. Chem.* **264**:21725–21736 (1989).
23. Abramson, J. J., and G. Salama. Critical sulfhydryls regulate calcium release from sarcoplasmic reticulum. *J. Bioenerg. Biomembr.* **21**:283–294 (1989).
24. Liu, G. H., and T. Oba. Change in surface charge of sarcoplasmic reticulum membrane may elicit conformational change in sulfhydryl groups of membrane proteins to release calcium. *Jpn. J. Physiol.* **39**:623–627 (1989).
25. Zimanyi, I., E. Buck, J. J. Abramson, M. M. Mack, and I. N. Pessah. Ryanodine induces persistent inactivation of the Ca^{2+} release channel from skeletal muscle sarcoplasmic reticulum. *Mol. Pharmacol.* **42**:1049–1057 (1992).
26. Sipple, T. O. New fluorochromes for thiols: maleimide and iodoacetimide derivatives of 3-phenylcoumarin fluorophore. *J. Histochem. Cytochem.* **29**:314–321 (1981).
27. Saito, A., S. Seiler, A. Chu, and S. Fleischer. Preparation and morphology of sarcoplasmic reticulum terminal cisternae from rabbit skeletal muscle. *J. Cell Biol.* **99**:875–885 (1984).
28. Lowry, O. H., N. J. Rosebrough, A. L. Farr, and R. J. Randall. Protein measurement with the Folin phenol reagent. *J. Biol. Chem.* **193**:265–275 (1951).
29. Laemmli, U. K. Cleavage of structural proteins during the assembly of the head of bacteriophage T_4. *Nature (Lond.)*. **227**:680–685 (1970).
30. Caswell, A. H., N. R. Brandt, J. P. Brunschwig, and S. Purkerson. Localization and partial characterization of the oligomeric disulfide-linked molecular weight 95,000 protein (triadin) which binds the ryanodine and dihydropyridine receptors in skeletal muscle triadic vesicles. *Biochemistry* **30**:7507–7513 (1991).
31. Airey, J. A., C. F. Beck, K. Murakami, S. J. Tanksley, T. J. Deerinck, M. H. Ellisman, and J. L. Sutko. Identification and localization of two triad junctional foot protein isoforms in mature avian fast twitch skeletal muscle. *J. Biol. Chem.* **265**:14187–14194 (1990).
32. Warren, G. B., P. A. Toon, N. J. M. Birdsall, A. G. Lee, and J. C. Metcalfe. Reconstitution of the calcium pump using defined membrane components. *Proc. Natl. Acad. Sci. USA* **71**:622–626 (1974).
33. Buck, E., I. Zimanyi, J. J. Abramson, and I. N. Pessah. Ryanodine stabilizes multiple conformational states of the skeletal muscle calcium release channel. *J. Biol. Chem.* **267**:23560–23567 (1992).
34. Brooks, S. P., and K. B. Storey. Bound and Determined: a computer program for making buffers of defined ion concentrations. *Anal. Biochem.* **201**:119–126 (1992).
35. Lai, F. A., M. Misra, L. Xu, H. A. Smith, and G. Meissner. The ryanodine receptor-Ca^{2+} release channel complex of skeletal muscle sarcoplasmic reticulum: evidence for a cooperatively coupled, negatively charged homotetramer. *J. Biol. Chem.* **264**:16776–16785 (1989).
36. Pessah, I. N., and I. Zimanyi. Characterization of multiple [^{3}H]ryanodine binding sites on the Ca^{2+} release channel of sarcoplasmic reticulum from skeletal and cardiac muscle: evidence for a sequential mechanism in ryanodine action. *Mol. Pharmacol.* **39**:679–689 (1991).
37. Morii, M., S. Danko, D. H. Kim, and N. Ikemoto. Fluorescence conformational probe study of calcium release from sarcoplasmic reticulum. *J. Biol. Chem.* **261**:2343–2348 (1986).
38. Ohkusa, T., J. J. Kang, M. Morii, and N. Ikemoto. Conformational change of the foot protein of sarcoplasmic reticulum as an initial event of calcium release. *J. Biochem. (Tokyo)* **109**:609–615 (1991).
39. Allen, G., and N. M. Green. Primary structure of cysteine-containing peptides from the calcium ion-transporting adenosine triphosphatase of rabbit sarcoplasmic reticulum. *Biochem. J.* **173**:393–402 (1978).
40. Mack, M. M., I. Zimanyi, and I. N. Pessah. Discrimination of multiple binding sites for antagonists of the calcium release channel complex of skeletal and cardiac sarcoplasmic reticulum. *J. Pharmacol. Exp. Ther.* **262**:1028–1037 (1992).
41. Knudson, C. M., K. K. Strong, C. R. Moomaw, C. A. Slaughter, and K. P. Campbell. Primary structure and topological analysis of junctional sarcoplasmic reticulum glycoprotein (triadin). *J. Biol. Chem.* **268**:12646–12654 (1993).
42. Brandt, N. R., A. H. Caswell, J. P. Brunschwig, J. J. Kang, B. Antoniu, and N. Ikemoto. Effects of anti-triadin antibody on Ca^{2+} release from sarcoplasmic reticulum. *FEBS Lett.* **299**:57–59 (1992).
43. Thieleczek, R., G. W. Mayr, and N. R. Brandt. Inositol polyphosphate-mediated repartitioning of aldolase in skeletal muscle triads and myofibrils. *J. Biol. Chem.* **264**:7349–7356 (1989).
44. Collins, J. H. Sequence analysis of the ryanodine receptor: possible association with a 12K, FK506-binding immunophilin/protein kinase C inhibitor. *Biochem. Biophys. Res. Commun.* **178**:1288–1290 (1991).
45. Orrenius, S., and G. Bellomo. Glutathione and calcium metabolism, in *Coenzymes and Cofactors, Vol. III, Glutathione: Chemical, Biochemical, and Medical Aspects* (D. Dolphin, R. Poulson, and O. Avramovic, eds.). Wiley, New York, 383–409 (1989).
46. Reed, D. J. Review of the current status of calcium and thiols in cellular injury. *Chem. Res. Toxicol.* **3**:495–502 (1990).
47. Palade, P. Drug-induced Ca^{2+} release from isolated sarcoplasmic reticulum. I. Use of pyrophosphate to study caffeine-induced Ca^{2+} release. *J. Biol. Chem.* **262**:6135–6141 (1987).

Send reprint requests to: Isaac N. Pessah, Department of Molecular Biosciences, Division of Pharmacology and Toxicology, School of Veterinary Medicine, University of California, Davis, CA 95616.